A Finite Element Study of Stable Crack Growth Under Plane Stress Conditions: Part I—Elastic-Perfectly Plastic Solids

R. Narasimhan
Research Fellow in Applied Mechanics.

A. J. Rosakis
Assistant Professor of Aeronautics and Applied Mechanics. Assoc. Mem. ASME

J. F. Hall
Assistant Professor of Civil Engineering.

Division of Engineering and Applied Science, California Institute of Technology, Pasadena, CA 91125

A detailed finite element study of stable crack growth in elastic-perfectly plastic solids obeying an incremental plasticity theory and the Huber-Von Mises yield criterion is performed under plane stress, small-scale yielding conditions. A nodal release procedure is used to simulate crack extension under continuously increasing external load. It is found that the asymptotic angular extent of the active plastic zone surrounding the moving crack tip is from $\theta = 0$ deg to about $\theta = 45$ deg. Clear evidence of an elastic unloading region following the active plastic zone is found, but no secondary (plastic) reloading is numerically observed. The near-tip angular stress distribution inside the active plastic zone is in good agreement with the variation inside a centered fan, as predicted by a preliminary asymptotic analysis by Rice. It is also observed that the stress components within the plastic zone have a strong radial variation. The nature of the near-tip profile is studied in detail.

1 Introduction

A slow, stable crack extension phase is often observed (Broek, 1968; Green and Knott, 1975) in elastic-plastic materials prior to catastrophic failure during which a steady increase in applied load is required to propagate the crack. The primary reason for this is the reduced singularity in the strains that results when the crack propagates into material that has already deformed plastically.

Several investigators have contributed in providing an understanding of the mechanics and the practical implications of stable crack growth by using both analytical and numerical techniques. Problems that have received wide attention are crack extension in elastic-perfectly plastic materials under the conditions of anti-plane shear and Mode I plane strain. Chitaley and McClintock (1971) constructed an asymptotic analytical solution for steady, quasi-static crack growth under anti-plane shear conditions. Following preliminary investigations by Rice (1968, 1975), Rice et al. (1980) assembled an asymptotic solution for cracks growing in an incompressible elastic-perfectly plastic material under Mode I plane strain. The solution for this problem was also found independently by Slepyan (1974) and Gao (1980). Finally, the asymptotic analysis of Drugan et al. (1982) accounted for crack growth under Mode I plane strain in elastic-perfectly plastic materials without the restriction of elastic incompressibility.

However, by contrast not many asymptotic solutions are available for cracks growing in strain-hardening materials, primarily due to the difficulty involved in the analytical treatment of the governing equations. Amazigo and Hutchinson (1977) performed an asymptotic analysis for steady-state crack extension in a linear hardening material under antiplane shear and Mode I plane strain and plane stress. Ponte Casteñeda (1987) has recently extended their analysis to include the possibility of secondary reloading and has also treated Mode II plane strain and plane stress. Nevertheless, some questions pertaining to Mode I plane strain and plane stress, in the limit as the perfect plasticity is approached, are left unanswered by his investigation (see for example Section 4 of the present paper). Also, Gao and Hwang (1981) performed a preliminary investigation about the near-tip fields for a crack growing in a material governed by a more realistic power hardening law.

Finite element studies simulating crack growth, by using nodal release procedure, were conducted by Sorensen (1978) under antiplane shear and by Sorensen (1979) and Sham (1983) under Mode I plane strain. Dean and Hutchinson (1980) and Lam and McMeeking (1984) have used a Eulerian finite element formulation to study steady-state crack advance in the above cases. On the other hand, remarkably little work has been performed regarding crack growth under Mode I plane stress, notwithstanding its practical importance, as, for example, to thin aircraft structures. Also, a study of plane stress crack gorwth is compelling, because of the possibility of direct comparison with experiments based on the optical method of caustics, which in recent years has showed great

Contributed by the Applied Mechanics Division for presentation at the Winter Annual Meeting, Boston, MA, December 13–18, 1987, of the American Society of Mechanical Engineers.

Discussion on this paper should be addressed to the Editorial Department, ASME, United Engineering Center, 345 East 47th Street, New York, N.Y. 10017, and will be accepted until two months after final publication of the paper itself in the JOURNAL OF APPLIED MECHANICS. Manuscript received by ASME Applied Mechanics Division, December 10, 1986; final revision May 21, 1987. Paper No. 87-WA/APM-20.

promise towards applications in ductile fracture (Rosakis and Freund, 1982; Zehnder et al., 1986). A preliminary analysis has been performed by Rice (1982), concerning the asymptotic nature of the stress and deformation fields near a growing crack tip in an elastic-perfectly plastic material under plane stress conditions. A complete (all-round) asymptotic solution for this problem has thus far remained elusive. Achenbach and Dunayevsky (1984) have recently investigated the variation of the plastic strain field along a ray ahead of the tip, based on the assumption of the validity of the asymptotic value for the stress field (Rice, 1982) up to the elastic-plastic boundary (see Section 4 for further discussion).

As far as numerical modelling is concerned, a steady-state Eulerian finite element study has been conducted recently by Dean (1983) for plane stress crack growth following the approach of Dean and Hutchinson (1980). However, as noted in Section 4 of this paper, the analysis of Dean (1983) is not very detailed, and certain issues pertaining to the near-tip stress and deformation fields have not been examined.

In the present investigation, a very detailed finite element study that provides great resolution near the crack tip has been carried out to model stable plane stress crack growth under continuous increase in external load, by using the nodal release procedure (Sorensen, 1979; Sham, 1983). Attention is restricted to elastic-perfectly plastic materials in the present analysis. This is a continuation of our earlier work (Narasimhan and Rosakis, 1986a), which analyzed the monotonic loading of a stationary crack under plane stress, small-scale yielding conditions.

2 Numerical Analysis

Formulation. The numerical modelling of the Mode I plane stress, small-scale yielding problem was discussed in detail by Narasimhan and Rosakis (1986a), who performed the analysis of a monotonically loaded stationary crack. In the present investigation, the results obtained by them will be used as initial conditions to simulate stable crack extension. Some of the features about the numerical analysis will be briefly outlined in this section. In the present paper $\{\mathbf{e}_1, \mathbf{e}_2, \mathbf{e}_3\}$ will represent an orthonormal frame centered at the crack tip and translating with it, while $\{\mathbf{e}_1', \mathbf{e}_2', \mathbf{e}_3'\}$ will be a fixed orthonormal frame situated at the position of the stationary crack tip.

The upper half of a domain R containing a crack and represented entirely by finite elements is shown in Figs. 1(*a*) and 1(*b*). The leading term in displacements of the linear elastic asymptotic solution,

$$u_\alpha = K_I \sqrt{\frac{r}{2\pi}} \hat{u}_\alpha(\theta), \tag{2.1}$$

was specified as a boundary condition on the outermost contour S of the domain.[1] The loading was applied through the Mode I stress intensity factor K_I or equivalently through the far-field value of the J integral. All plastic deformation was contained within a distance from the crack tip, which was less than 1/30 of the radius of S.

The active region of Fig. 1(*a*) has a total of 1704 four-noded quadrilateral elements and 3549 degrees of freedom. The quadrilaterals were formed from four constant strain triangles with static condensation of the internal node. Static condensation was also employed in the large region surrounding the active mesh, which always remained elastic. The cutout of Fig. 1(*a*), which is a fine mesh region near the crack tip, is shown in detail in Fig. 1(*b*). The small square elements near the crack tip have a size L, which is about 1/385 of the radius R_A of the active region and about 1/3400 of the radius of S.

[1] Throughout this paper, Greek subscripts will have range 1,2, while Latin subscripts will take values 1,2,3.

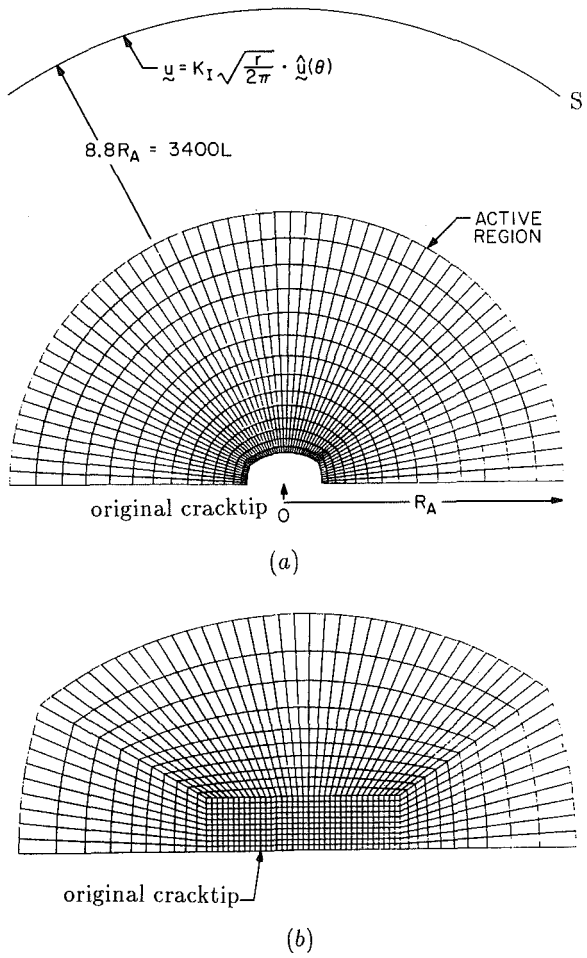

Fig. 1 Finite element mesh: (*a*) outer mesh; (*b*) fine mesh near the crack tip

Constitutive Assumptions. The material model that was considered here was that of an isotropic elastic-perfectly plastic solid. A small strain incremental plasticity theory was employed along with the Huber-Von Mises yield condition and the associated flow rule. The total strain rate tensor is assumed to be decomposed into elastic and plastic parts, and the constitutive law for material currently experiencing plastic deformation is given by,

$$\dot{\sigma}_{ij} = C^*_{ijkl}\dot{\epsilon}_{kl} = \left[C_{ijkl} - \frac{C_{ijpq}S_{pq}S_{mn}C_{mnkl}}{S_{rt}C_{rtuv}S_{uv}}\right]\dot{\epsilon}_{kl}. \tag{2.2}$$

Here C_{ijkl} is the isotropic, positive definite elasticity tensor, and S_{ij} is the deviatoric stress tensor. In the present analysis, the yield criterion and the constitutive law (2.2) were used along with the plane stress condition,

$$\sigma_{3i} \equiv 0. \tag{2.3}$$

On using equation (2.3) in equation (2.2), a constraint for $\dot{\epsilon}_{33}$ in terms of $\dot{\epsilon}_{\alpha\beta}$ can be obtained. The ratio of the Young's modulus to the yield stress in pure shear (E/τ_0) was taken as 350 and the Poisson's ratio (ν) as 0.3 in the computation.

Finite Element Scheme. A displacement based finite element method was employed and inertia effects were neglected in the analysis. The incremental finite element equilibrium equations were derived from the principle of virtual work by

linearization (Bathe, 1982). These equations were solved for each time step using the iterative Newton-Raphson method. An explicit integration procedure also known as the Tangential Predictor-Radial Return method (Schreyer et al., 1979) was employed together with subincrementation to integrate the incremental stress-strain law.

Solution Strategy. The plastic zone at the end of the stationary load history had a maximum extent, which occurred ahead of the crack tip, of about 100 times the smallest element size L. Subsequently, twenty one-element crack growth steps were simulated using the nodal release procedure, as described below. The stiff spring that was attached to the crack tip node in the x_2 direction, in order to enforce the symmetry condition ($u_2 = 0$), was removed and was replaced by the point load acting on it. This point load was subsequently relaxed to zero in twenty increments, at the end of which a traction-free element surface emerged, and the crack advanced by one element length L.

The externally applied load through the far-field J integral (or K_I) was increased simultaneously during the above nodal release procedure (as done by Sham, 1983), in order to model stable crack extension in a continuous manner. During crack growth the K field remained centered at the location of the original crack tip. This was because while the K field was specified at a radius of 3400L, the crack advanced by only 20L. For this purpose, a simple J versus crack growth (Δa) history with a constant slope was used. Following eighteen one-element crack growth steps at $T \equiv (E/\sigma_0^2) dJ/da = 5$, two crack growth steps at four different T values of 0, 5, 15, and 20 were simulated (T is the nondimensional Paris tearing modulus). The last two steps were thus carried out in order to study the effect of different rates of increase of external load on crack displacement increment. The computation was performed using a Cray XMP (Boeing Computer Services, Seattle). The total CPU time taken was about 3 CPU hours.

3 Asymptotic Fields Near Propagating Crack Tips

Plane Strain. Rice et al. (1980) assembled a near-tip solution for quasi-static crack advance under plane strain in an incompressible material ($\nu = 0.5$). This solution is essentially the Prandtl field (Rice, 1968) together with an elastic unloading sector following the centered fan. This was added to eliminate the negative plastic work that would otherwise occur at the trailing boundary of the fan. The asymptotic form of the plastic strains in the fan is given by,

$$\epsilon^p_{\alpha\beta} \sim \frac{(5-4\nu)}{2\sqrt{2}} \frac{\tau_0}{E} G_{\alpha\beta}(\theta) ln\left(\frac{\bar{R}}{r}\right), \quad r \to 0. \tag{3.1}$$

where $\bar{R}$ is an arbitrary length scale. The angular factors $G_{\alpha\beta}(\theta)$ are fully determined from an asymptotic angular integration of the plastic strain rates (Rice, 1982). It should be noted that the dominant log(r) term of (3.1) is much weaker than the $1/r$ plastic strain singularity near a monotonically loaded stationary crack tip (Rice, 1968).

Motivated by the above, Rice et al. (1980) proposed the following form for the near-tip crack opening rate during stable plane strain crack advance,

$$\dot{\delta} \sim \frac{\alpha \dot{J}}{\sigma_0} + \beta \frac{\sigma_0}{E} \dot{a} ln\left(\frac{R}{r}\right), \quad r \to 0. \tag{3.2}$$

In the above, α and β are constants and R is a length dimension, which is expected to scale with the plastic zone size under small-scale yielding conditions, so that

$$R = s\left(\frac{EJ}{\sigma_0^2}\right). \tag{3.3}$$

Here, J is the remotely applied value of the J integral which, under small scale yielding conditions, is given by,

$$\begin{aligned} J &= (1-\nu^2)\frac{K_I^2}{E} \quad \text{(plane strain)} \\ &= \frac{K_I^2}{E} \quad \text{(plane stress).} \end{aligned} \tag{3.4}$$

The constant β in (3.2) can be obtained from an all-round asymptotic solution (Rice et al., 1980; Drugan et al., 1982), whereas the constants α in (3.2) and s in equations (3.3) are undetermined from the asymptotic analysis.

The second term in (3.2) arises because of the log(r) dominant singularity in the material particle velocities. The first term in (3.2) encompasses the assumption that the higher-order terms in velocities are bounded and linear in load rate ($\dot{J}$ for small scale yielding). Also, for $\dot{a} = 0$, the right-hand side of (3.2) reduces to the correct expression for the discrete crack opening rate that is observed during the monotonic loading of a stationary crack. An asymptotic integration of (3.2) can be carried out to obtain the near-tip crack opening displacement during stable crack growth (when crack length a increases continuously with J) as follows,

$$\delta \sim \frac{\alpha r}{\sigma_0} \frac{dJ}{da} + \beta r \frac{\sigma_0}{E} ln\left(\frac{eR}{r}\right), \quad r \to 0, \tag{3.5}$$

where e is the base of the natural logarithm. As opposed to the monotonic loading of a stationary crack, equation (3.5) implies that the opening displacement at the crack tip is equal to zero during crack growth. However, as can be noticed from (3.5), the crack profile during growth exhibits a vertical tangent at the tip.

Plane Stress. The general features outlined above for plane strain apply to plane stress as well, with some modifications. No all-round asymptotic solution that satisfies all the boundary and symmetry conditions and that does not violate material stability postulates has yet been assembled for this case. However, Rice (1982) has performed a preliminary asymptotic analysis and has demonstrated that only two types of plastic sectors can exist near the crack tip. These are centered fan sectors in which radial lines are stress characteristics ($s_{rr} \equiv 0$) and constant stress sectors in which the Cartesian components of stress $\sigma_{\alpha\beta}$ are constant (not functions of angle θ). The asymptotic stress and deformation fields within the above plastic sectors and in elastic unloading sectors have been derived by Rice (1982).

The asymptotic stress field within a centered fan sector is summarized below assuming that it adjoins the $\theta = 0$ ray (similar to the stationary crack tip solution of Hutchinson, 1968):

$$\sigma_{rr} = \tau_0 \cos\theta, \ \sigma_{\theta\theta} = 2\tau_0 \cos\theta, \ \sigma_{r\theta} = \tau_0 \sin\theta, \ r \to 0 \tag{3.6}$$

Rice (1975) has demonstrated that if a centered fan adjoins the $\theta = 0$ line, then the plastic strains in front of the crack tip are given by:

$$\epsilon^p_{ij} = \frac{1}{2} \frac{\tau_0}{E} G_{ij} ln^2\left(\frac{\bar{R}}{r}\right), \ \theta = 0, \quad r \to 0, \tag{3.7}$$

where,

$$\left.\begin{aligned} G_{11} &= 0 \quad G_{12} = 0 \\ G_{22} &= 2 \quad G_{33} = -2 \end{aligned}\right\}. \tag{3.8}$$

It should be observed that the plastic strains (on the $\theta = 0$ ray) are singular as $\log^2(r)$ in plane stress, whereas in plane strain the plastic strains in the fan have a log(r) dominant singularity from (3.1). The stronger $\log^2(r)$ dominant plastic strain singularity in plane stress (which also occurs in antiplane shear) arises because the crack propagates into a centered fan region unlike in Mode I plane strain.

In plane stress, the material particle velocities have a log(r) singularity analogous to plane strain (see Rice, 1982). Hence one expects the crack opening rate during stable plane stress crack advance to have the same functional form as (3.2). Also

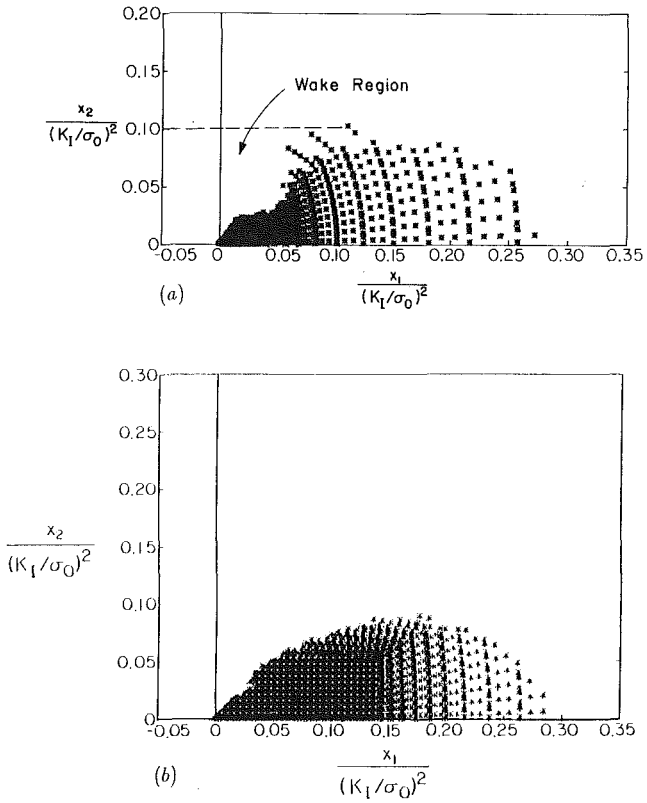

Fig. 2(a) Active plastic zone surrounding the propagating crack tip; (b) plastic zone corresponding to the stationary crack (Narasimhan and Rosakis, 1986a)

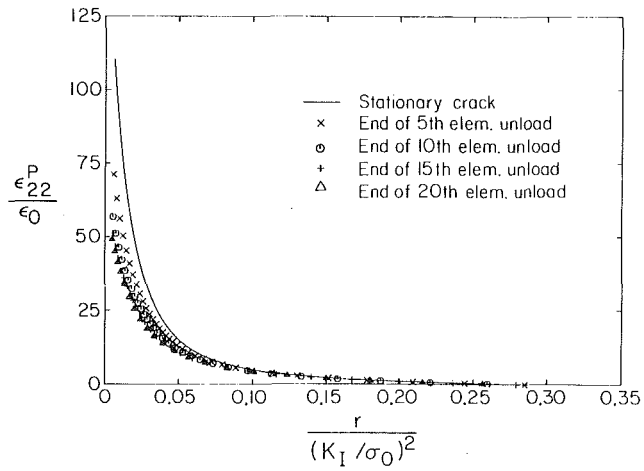

Fig. 3 Radial distribution of plastic strain ahead of the propagating crack tip for various levels of crack growth

the equations from (3.2) to (3.5) and the accompanying discussions are expected to apply for stable plane stress crack growth.

4 Results and Discussion

Plastic Zone. The active plastic zone surrounding the crack tip is shown in Fig. 2(*a*) in moving coordinates that have been made dimensionless by the parameter $(K_I/\sigma_0)^2$. For comparison purposes, the plastic zone corresponding to a stationary crack under plane stress conditions, which was obtained by Narasimhan and Rosakis (1986a), is shown in Fig. 2(*b*). In Fig. 2(*a*), the current crack tip is at the origin of the coordinate system, and this result was obtained at the end of twentieth crack growth step. A point in the figure represents an actively yielding integration station (currently on the yield surface in stress space) within an element. It can be seen from the figure that a large elastic unloading region follows the active plastic zone. The active plastic zone appears to occupy an asymptotic angular extent from $\theta = 0$ deg to about 45 deg, which will be verified later.

The elements behind the active plastic zone, which are close to the crack plane and which occupy the angular range from $\theta = 45$ to 180 deg, have unloaded elastically. These elements have previously experienced plastic yielding during the passage of the crack tip. The present numerical solution does not exhibit any secondary (plastic) reloading along the crack flank. This is in contrast to plane strain, where a secondary plastic region was found, extending behind the moving crack tip (Sham, 1983).

As can be seen from Fig. 2(*a*), the trailing boundary of the active plastic zone seems to have a kink, resulting in a shape similar to that observed in antiplane shear (Sorensen, 1978; Dean and Hutchinson, 1980). The parallel between plane stress and antiplane shear has been recognized earlier, from the presence of an intense deformation zone (centered fan) ahead of the moving tip in both cases. In the present computation, the kink in the active plastic zone developed during the first few crack growth steps and persisted with subsequent crack advance. Also, the overall features of the plastic zone did not change much after the first few crack growth steps.

The maximum radial extent of the plastic zone, which occurs directly ahead of the growing crack tip ($\theta = 0$), is $R_p \approx 0.28(K_I/\sigma_0)^2$, which is about the same as the stationary problem (Fig. 2(*b*)). Also, on comparing Figs. 2(*a*) and 2(*b*), it can be seen that the plastic zone for the propagating crack is similar in overall shape and size to that obtained for the stationary problem at points away from the crack tip. However, near the tip the two plastic zones seem to deviate in shape, primarily due to elastic unloading behind the trailing boundary during crack growth. As pointed out by Rice (1982), strong changes in plastic zone shape near the tip and a tendency to reestablish a shape similar to that for the stationary crack at points away from the tip are expected during the initial stages of crack growth. This can also be observed in the results for both antiplane shear (e.g., Sorensen, 1978) and plane strain (e.g., Sham, 1983).

Finally, it is noted that the plastic zone of Fig. 2(*a*) compares well with the steady-state result obtained by Dean (1983), from a Eulerian finite element formulation, except for the presence of the kink. However, the present finite element solution is more detailed, since it has a larger ratio of plastic zone to smallest element size of over 100 as compared to about 35 in Dean's computation. Also, unlike Dean's work, the initial phase of crack growth was simulated here under continuously increasing external load.

Radial Distribution of Plastic Strain. The radial distribution of normalized plastic strain, $\epsilon_{22}^p/\epsilon_0$, with respect to normalized distance, $r/(K_I/\sigma_0)^2$, ahead of the current crack tip is shown in Fig. 3. Results are presented for various levels of crack growth under steadily increasing value of far-field J at $T = 5$. The solid line in the figure is the plastic strain distribution ahead of a monotonically loaded stationary crack tip, which was obtained by Narasimhan and Rosakis (1986a). It can be seen that the plastic strain converges rapidly during the first few crack growth steps to an invariant distribution. For example, at a distance of $0.01(K_I/\sigma_0)^2$ ahead of the moving crack tip, the plastic strain dropped by 32 percent during the first five crack growth steps and by 17 percent, 8 percent, and 3 percent during the sixth to tenth steps, eleventh to fifteenth steps, and sixteenth to twentieth steps, respectively. Such rapid convergence was also observed in the numerical simulation of antiplane shear crack growth by Sorensen (1978).

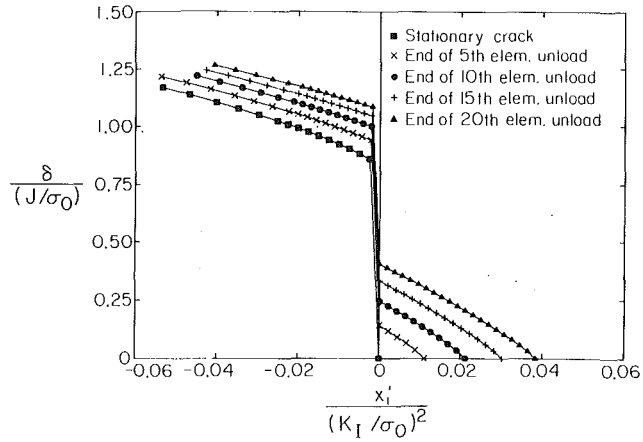

Fig. 4 Development of crack profile for various levels of crack growth

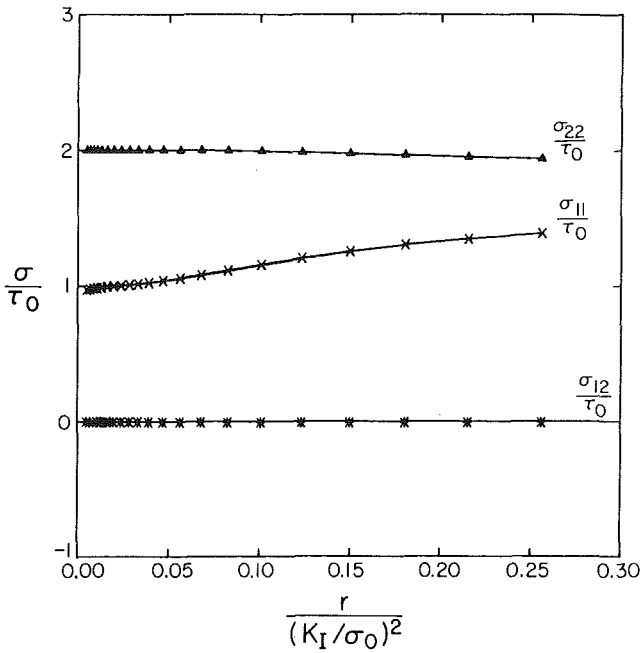

Fig. 5 Radial distribution of stresses ahead of moving crack tip

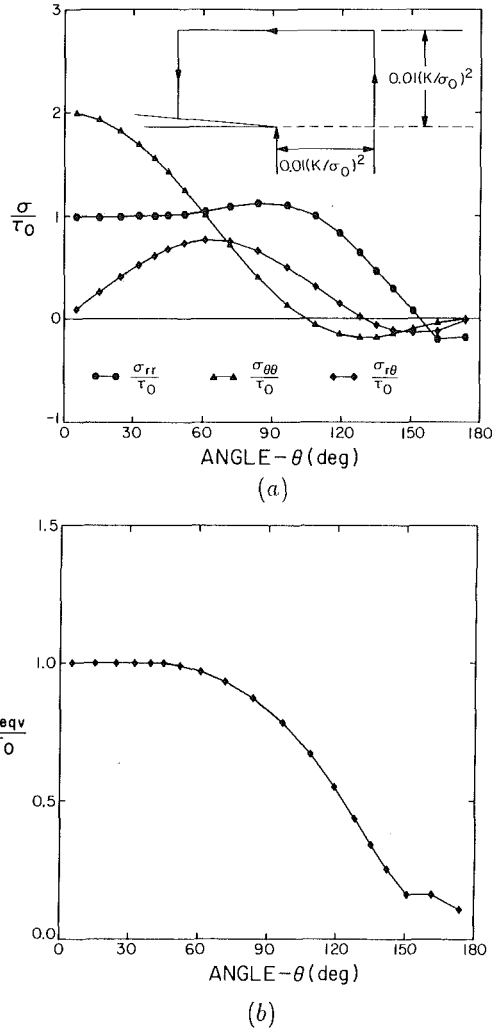

Fig. 6 Near-tip angular distribution of (a) normalized polar stress components and (b) Von Mises equivalent stress

As can be seen from Fig. 3, the plastic strain distribution ahead of the tip during growth exhibits a weaker singularity than in the stationary problem. This fact is the origin for the stable crack extension phase (McClintock and Irwin, 1965) observed in elastic-plastic materials (preceding instability), when crack growth occurs under steadily increasing external load.

Crack Profiles. The development of the crack opening profile for various levels of crack growth at $T=5$ is shown in Fig. 4 in the nondimensional form $\delta/(J/\sigma_0)$ versus $x_1'/(K_I/\sigma_0)^2$. The stationary crack profile is also plotted in the figure for comparison. As can be seen from the figure, the crack profile changes from a blunted form at the end of the stationary load history to a sharp shape during crack growth. This is because of the lessened strain concentration that results when the crack propagates into material that has already deformed plastically. In Section 5 this numerically obtained profile will be used to estimate the parameters α, β, and s in the asymptotic equation (3.5).

Radial Distribution of Stresses. The radial variation of the normalized stress components, $\sigma_{\alpha\beta}/\tau_0$, versus normalized distance ahead of the crack tip at the end of the twentieth release step is shown in Fig. 5. The centroidal values of stresses in the row of elements ahead of the tip have been used to construct this plot. The numerically obtained stresses very near the crack tip approach the asymptotic distribution given by equation (3.6) which assumes that there is a centered fan ahead of the tip. For example, from the finite element results at $r=0.01(K_I/\sigma_0)^2$, the values of σ_{11} and σ_{22} are $0.99\tau_0$ and $1.999\tau_0$, in excellent agreement with the values τ_0 and $2\tau_0$, respectively, given by (3.6).

It can be seen from Fig. 5 that the σ_{11} stress component exhibits a strong radial variation with a value of $1.40\tau_0$ at the elastic-plastic boundary. The value of σ_{11} differs from the asymptotic limit by less than 5 percent in the range $r<0.04(K_I/\sigma_0)^2$. This stress variation compares closely with that for the stationary crack (Narasimhan and Rosakis, 1986a). As noted by them, it suggests possible curving of the leading boundary of the fan at moderate distances from the tip. This will also be discussed later in connection with Fig. 7.

Near-Tip Angular Distribution of Stresses. The angular variation of the normalized polar stress components at a distance of $0.01(K_I/\sigma_0)^2$ from the moving crack tip (which is within $0.04R_p$) is shown in Fig. 6(*a*). The centroidal values of stresses in the elements lying on a rectangular contour surrounding the moving crack tip, which is shown as an inset in the figure, have been used to construct this plot. The angular variation along the above contour of the Von Mises equivalent stress, $\sigma_{eqv}=(3/2s_{ij}s_{ij})^{1/2}$ which has been normalized by σ_0, is shown in Fig. 6(*b*).

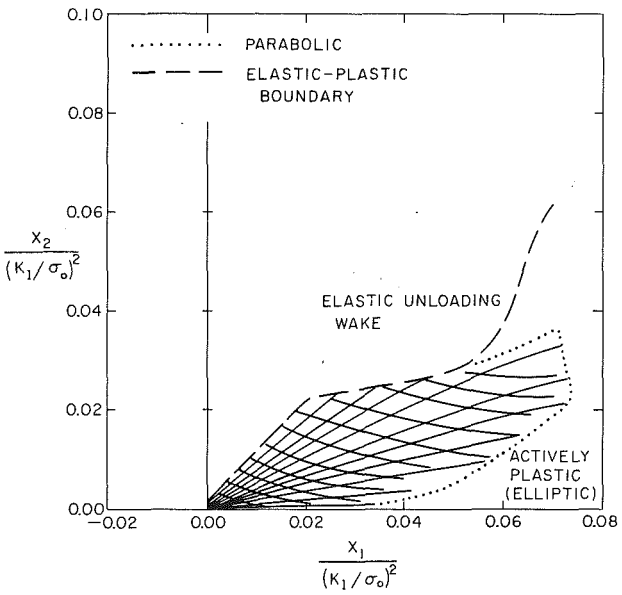

Fig. 7 Stress characteristics within active plastic zone

As can be seen from Fig. 6(*b*), σ_{eqv} becomes less than σ_0 for $\theta > 45$ deg, which suggests that the asymptotic angular extent of the active plastic zone is about 45 deg. This agrees well with visual observation of Fig. 2(*a*). However, from published results for crack advance under both antiplane shear (e.g., Dean and Hutchinson, 1980) and plane strain (e.g., Sham, 1983), where the asymptotic angular extent of active yielding was overestimated by finite element solutions, one is led to interpret the above conclusion with some caution. Also, from Fig. 6(*b*), it can be seen that σ_{eqv} does not become equal to σ_0 as θ approaches 180 deg, which implies that no secondary (plastic) reloading has been detected by this numerical solution.

The angular distribution of stresses (Fig. 6(*a*)) within the actively yielding region is in good agreement with the variation in a centered fan, as predicted by equation (3.6). For example, in the angular range 0 deg $\leq \theta <$ 45 deg, the values of $\sigma_{\theta\theta}$ and $\sigma_{r\theta}$ as given in Fig. 6(*a*) differ from that obtained using equation (3.6) by less than 1 percent and 4 percent, respectively. However, the value of σ_{rr} shown in Fig. 6(*a*) agrees with that given by equation (3.6) to within 8 percent in the angular range 0 deg $\leq \theta \leq 25$ deg and deviates substantially for 25 deg $< \theta <$ 45 deg. The reason for this discrepancy will be explained later in this section. Also, the angular stress distribution of Fig. 6(*a*) compares quite well with the finite element results of Dean (1983). However, as pointed out earlier, the present computation is considered to be more detailed than Dean's analysis.

The recent asymptotic analysis of Ponte Castañeda (1987) for steady, quasi-static crack growth in a linear hardening material is unfortunately not definitive about the asymptotic angular extent of the primary plastic zone in the limit as the perfect plasticity case is approached. He obtains a primary plastic angle of about 53.2 deg and 49 deg when the ratio E_t/E of the tangent modulus to the elastic modulus is 0.001 and 0.0001, respectively. Also the presence of a secondary reloading zone and its angular extent (which is extremely small) are not completely conclusive from his results, in the limit as E_t/E tends to be zero. The prediction of a very small reloading angle is, however, not inconsistent with the present numerical results, since such a tiny reloading zone cannot possibly be detected by a finite element scheme.

Nevertheless, the angular factors $\sigma_{ij}(\theta)$ of the dominant r^s term for the stresses given by Ponte Castañeda (1987) for $E_t/E = 0.001$ agree closely with the present numerical solution of Fig. 6, except for the σ_{rr} component, which seems to deviate in the angular range from $\theta = 25$ deg to about 100 deg. Also, the stress distribution obtained by Ponte Castañeda (1987) for $E_t/E = 0.001$ suggests yielding in compression for θ very close to 180 deg. While the present results do indicate a region near the crack flank where σ_{rr} is negative (see Fig. 6), no yielding in compression has been observed.

Stress Characteristics. The two families of stress characteristics within the active plastic zone, near the propagating crack tip, are shown in Fig. 7, using nondimensional crack tip coordinates. The dashed line in the figure is the boundary of the active plastic zone. The stress characteristics were plotted using the averaged stresses within the elements, as described by Kachanov (1974). These characteristics are lines along which the direct component of the stress deviator vanishes. The dotted line in the figure separates a region near the tip, in which the equations for the stresses are hyperbolic, from a region outside, in which they are elliptic. At each point on the dotted line, the condition for parabolicity of the governing equations for the stresses (see Kachanov, 1974) is satisfied. As can be seen from the figure, the two families of characteristics become mutually tangential to each other at every point along this dotted line, as it curves upwards from the $\theta = 0$ ray. However, it is not clear whether the elliptic region extends all the way up to the crack tip as a wedge of vanishingly small angular extent, as $r \to 0$ along the $\theta = 0$ ray, although there is some evidence to suggest this possibility. This observation might explain the difficulties encountered in constructing an all-around solution based on the asymptotic equations of Rice (1982).

Two important observations should be made from this figure. Firstly, it can be seen that a family of characteristics focusses at the crack tip in the angular range from $\theta = 0$ deg to about 25 deg, beyond which the characteristics seem to intersect the crack plane slightly behind the tip. This is probably because of the fact that, due to discretization, the crack tip is not precisely sensed in the finite element solution leading, according to the terminology of Sorensen (1978), to a "fuzzy crack tip phenomenon."

This was also observed in antiplane shear by Dean and Hutchinson (1980), who found that the active plastic zone obtained from their steady-state finite element solution extended from $\theta = 0$ deg to about 60 deg, while the charcteristics focussed at the tip only for angles less than 20 deg. For comparison, the analytical asymptotic solution of Chitaley and McClintock (1971) in antiplane shear crack growth has a centered fan region from $\theta = 0$ deg to 19.69 deg, followed by a large elastic unloading region and a tiny secondary reloading zone.

Secondly, the radial family of charcteristics in Fig. 7 bend downwards (towards the $\theta = 0$ ray) even for small distances ($r > 0.01(K_I/\sigma_0)^2$) from the tip. These two factors probably account for the strong discrepancy in the σ_{rr} stress component, between the finite element solution and the analytical asymptotic expression equation (3.6), in the angular range 25 deg $< \theta <$ 45 deg.

Finally, the strong radial variation in the stresses ahead of the crack tip (Fig. 5), combined with the observation of the change in nature of the governing equations as the distance from the crack tip is increased (Fig. 7), seems to disagree with the assumption of a constant stress field ahead of the tip made by Achenbach and Dunayevsky (1984).

5 Study of the Propagating Crack Profile

In this section, a value for the parameter β in the asymptotic crack opening rate (3.4) will be obtained by fitting the analytical asymptotic form to the numerically obtained values. The method employed is similar to that used by Sham (1983) in stable plane strain crack advance. Also, the linearity of the

higher-order term in (3.4) with respect to $\dot{J}$ will be verified from the numerical solution.

To that effect, the crack opening rate $\dot{\delta}$ is written as

$$\dot{\delta} \sim \dot{a}\frac{\sigma_0}{E}\left[f\left(\frac{a}{L}\right)+\beta ln\left(\frac{L}{r}\right)\right], \quad r\to 0, \tag{5.1}$$

where L is the smallest element size and is a convenient length scale and a is the crack length. Under small-scale yielding conditions, the function $f(a/L)$ can be shown to have the following form (see Section 3 and also Rice et al., 1980; Sham, 1983),

$$f\left(\frac{a}{L}\right)=g(T(a))+\beta ln\left(\frac{EJ(a)/\sigma_0^2}{L}\right), \tag{5.2}$$

where the quantity EJ/σ_0^2 has the dimension of length and is a measure of the plastic zone size. In the above equation, J, which is the remotely applied value of the J integral, and the nondimensional Paris tearing modulus $T=(E/\sigma_0^2)(dJ/da)$ are functions of the crack length a. If $g(T)$ is a linear function of T as was assumed in Section 3, then comparison of equation (5.2) with equations (3.2) and (3.3) gives

$$g(T)=\alpha T+\beta ln s, \tag{5.3}$$

where α and s will be taken as constants for limited amounts of crack growth.

The crack displacement increment at a fixed material point $(x_1',0)$, when the crack grows from a_1 to a_2, can be obtained by integrating (5.1) as follows (Sham, 1983),

$$\frac{E}{\sigma_0}\frac{\Delta\delta(x_1',a)}{L}\sim\Delta F+\beta\left[\frac{a_2-x_1'}{L}ln\left(\frac{eL}{a_2-x_1'}\right)-\frac{a_1-x_1'}{L}ln\left(\frac{eL}{a_1-x_1'}\right)\right]. \tag{5.4}$$

In the above equation, e is the base of the natural logarithm and

$$\left.\begin{aligned}\Delta\delta(x_1',a)&=\delta(x_1',a_2)-\delta(x_1',a_1)\\ \Delta F&=\int_{a_1/L}^{a_2/L}f(\zeta)d\zeta\end{aligned}\right\}. \tag{5.5}$$

The values of β and ΔF were obtained as the slope and axis intercept of a least-squares straight line fit to

$$\frac{E}{\sigma_0}\left(\frac{\Delta\delta(x_1',a)}{L}\right) \text{ versus } \Delta\left[\frac{a-x_1'}{L}ln\left(\frac{eL}{a-x_1'}\right)\right]$$

for successive one-element crack growth steps.

The representative straight line fits for crack growths under four different values of T of 0, 5, 15, and 20, which were simulated for the twentieth release step, is shown in Fig. 8. The first node behind the crack tip has been omitted and the data corresponding to the next five nodes have been plotted in this graph. The first node was omitted because it was observed that the crack tip element undergoes excessive rotation during the nodal release procedure. This conclusion was reached by performing a sensitivity study as described below. The average value of β based on the first six nodal points behind the crack tip was obtained as 2.1. On omitting the first node, it was found that a better straignt line fit can be made to the data corresponding to the net five nodal points (as in Fig. 8), which, however, gave a substantially lower average value of β of 1.7. The straight line fits underwent very little change on omitting the first and second nodes behind the tip, giving an average value of β of 1.67. On the basis of the above study, it is concluded that correct estimate for β, based on the crack displacement increments obtained from the finite element solution is around 1.70.

The value of ΔF obtained from the axis intercept can be taken approximately as

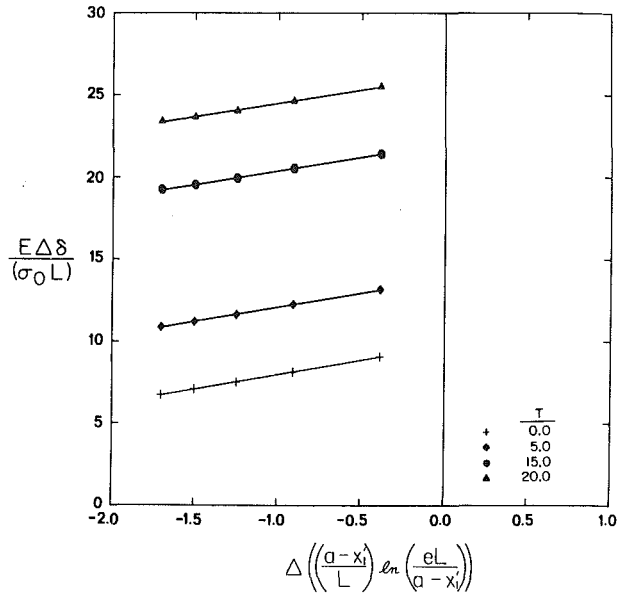

Fig. 8 Straight line fits to normalized crack displacement increments during the twentieth release step to determine β in asymptotic equation for crack opening rate

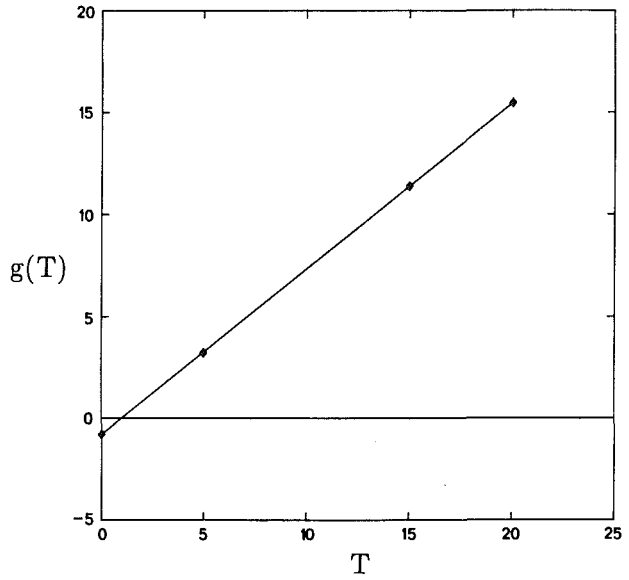

Fig. 9 Variation of higher-order term $g(T)$ in crack opening rate with respect to T. Straight line fit has been made to determine α and s.

$$\Delta F\approx\frac{(a_2-a_1)}{L}f\left(\frac{\bar{a}}{L}\right), \tag{5.6}$$

where $\bar{a}=(a_1+a_2)/2$. The value of $f(\bar{a}/L)$, which was computed from the above equation, was used along with the mean value of J during crack growth from a_1 to a_2 in equation (5.2) to determine $g(T)$. The values of $g(T)$ obtained as above for crack growth simulations under four different values of T during the twentieth release step are plotted against T in Fig. 9. It can be seen that a very accurate straight-line fit can be made to the numerically obtained points validating the assumption of linearity of $g(T)$ with respect to T made in Section 3.

On employing equation (5.3) (with β as 1.7), the values of α and s were obtained as 0.82 and 0.60 from the slope and axis intercept of the straight line fit (Fig. 9), respectively. From the analysis that included the first node behind the crack tip to determine β and ΔF (giving β as 2.1), the values of α and s were estimated as 0.82 and 0.24, respectively.

The value of α computed above is thus completely insensitive to the determination of β and is also in good agreement with the corresponding estimate from the opening displacement of the stationary crack, which was 0.85 as reported by Narasimhan and Rosakis (1986a). The value of s, on the other hand, seems to be extremely sensitive to the accuracy in determining β. This can also be observed in plane strain from the scatter in published numerical results for β and s (e.g., Sham, 1983; Dean and Hutchinson, 1980; Lam and McMeeking, 1984.

Finally, the asymptotic crack profile as given by (3.5) is plotted in nondimensional form for crack growth at $T=5.0$ in Fig. 10 with the parameters α, β and s taken as 0.82, 1.7, and 0.6, respectively. The values obtained from the finite element solution are also plotted in the figure for comparison. It is found that the predicted asymptotic crack profile is very close to the numerical solution in the range $r<0.04(K_I/\sigma_0)^2$.

A discussion of the implementation of a ductile fracture criterion will be presented in Part II of this investigation. This study will also result in the prediction of plane stress resistance curves for the case of perfect plasticity.

Acknowledgment

The authors would like to express their gratitude to Professor J. K. Knowles for his valuable advice and encouragement. This investigation was supported by the Office of Naval Research through ONR contract #N00014-85-K-0596. The computations were performed using the Supercomputer at Boeing Computer Services, Seattle. This was made possible through NSF contract #MEA-8307785. The above contracts and the facilities provided by Boeing Computer Services are gratefully acknowledged.

References

Achenbach, J. D., and Dunayevsky, V., 1984, "Crack Growth under Plane Stress Conditions in an Elastic Perfectly-Plastic Material," *Journal of Mechanics and Physics of Solids*, Vol. 32, pp. 89–100.

Amazigo, J. C., and Hutchinson, J. W., 1977, "Crack-Tip Fields in Steady Crack Growth with Linear Strain-Hardening," *Journal of Mechanics and Physics of Solids*, Vol. 25, pp. 81–97.

Bathe, K. J., 1982, *Finite Element Procedures in Engineering Analysis*, Prentice Hall, Englewood Cliffs, New Jersey.

Broek, D., 1968, "Some Considerations on Slow Crack Growth," *International Journal of Fracture*, Vol. 4, pp. 19–34.

Ponte Castañeda, P. P., 1987, "Asymptotic Fields in Steady Crack Growth with Linear Strain-Hardening," *Journal of Mechanics and Physics of Solids*, Vol. 35, pp. 227–268.

Chitaley, A. D., and McClintock, F. A., 1971, "Elastic-Plastic Mechanics of Steady Crack Growth Under Anti-Plane Shear," *Journal of Mechanics and Physics of Solids*, Vol. 19, pp. 147–163.

Dean, R. H., 1983, "Elastic-Plastic Steady Crack Growth in Plane Stress," *Elastic-Plastic Fracture: Second Symposium; Volume I—Inelastic Crack Analysis*, ASTM STP 803, American Society for Testing and Materials, pp. I-39–I-51.

Dean, R. H., and Hutchinson, J. W., 1980, "Quasi-Static Steady Crack Growth in Small-Scale Yielding," *Fracture Mechanics: Twelfth Conference*, ASTM STP 700, American Society for Testing and Materials, pp. 383–405.

Drugan, W. J., and Rice, J. R., 1984, "Restrictions on Quasi-Statically Moving Surfaces of Strong Discontinuity in Elastic-Plastic Solids," *Mechanics of Material Behavior*, Dvorak, G. J., and Shield, R. T., eds., Elsevier, Amsterdam, pp. 59–73.

Drugan, W. J., Rice, J. R., and Sham, T. L., 1982, "Asymptotic Analysis of Growing Plane Strain Tensile Cracks in Elastic-Ideally Plastic Solids," *Journal of Mechanics and Physics of Solids*, Vol. 30, pp. 447–473.

Gao, Y. C., 1980, "Elastic-Plastic Fields at the Tip of a Crack Growing Steadily in a Perfectly Plastic Medium," *Acta Mechanica Sinicia*, in Chinese, No. 1, pp. 48–56.

Gao, Y. C., and Hwang, K. C., 1981, "Elastic-Plastic Fields in Steady Crack Growth in a Strain Hardening Material," *Proceedings of the Fifth International Conference on Fracture*, Francois, D., ed., Pergamon Press, New York, Vol. 2, pp. 669–682.

Green, G., and Knott, J. F., 1975, "On Effects of Thickness on Ductile Crack Growth in Mild Steel," *Journal of Mechanics and Physics of Solids*, Vol. 23, pp. 167–183.

Hutchinson, J. W., 1968, "Plastic Stress and Strain Fields at a Cracktip," *Journal of Mechanics and Physics of Solids*, Vol. 16, pp. 337–347.

Kachanov, L. M., 1974, *Fundamentals of the Theory of Plasticity*, Mir Publishers, Moscow, pp. 244–262.

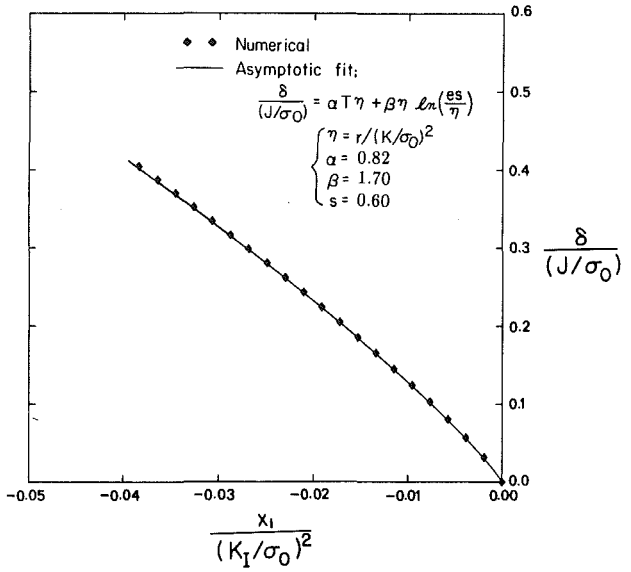

Fig. 10 Comparison of predicted asymptotic crack (solid line) with the finite element solution for stable crack growth at $T=5.0$

Lam, P. S., and McMeeking, R. M., 1984, "Analysis of Steady Quasistatic Crack Growth in Plane Strain Tension in Elastic-Plastic Materials with Non-Isotropic Hardening," *Journal of Mechanics and Physics of Solids*, Vol. 32, pp. 395–414.

McClintock, F. A., and Irwin, G. R., 1965, "Plasticity Aspects of Fracture Mechanics," *Fracture Toughness Testing and its Applications*, ASTM STP 381, pp. 84–113.

Narasimhan, R., and Rosakis, A. J., 1986a, "A Finite Element Analysis of Small-Scale Yielding near a Stationary Crack Under Plane Stress," Caltech Report SM 86-21, Pasadena, CA, *Journal of Mechanics and Physics of Solids*, to appear, 1988.

Narasimhan, R., and Rosakis, A. J., 1986b, "Reexamination of Jumps across Quasistatically Propagating Surfaces Under Generalized Plane Stress in Anisotropically Hardening Elastic-Plastic Solids," Caltech Report SM 86-3, Pasadena, CA, ASME *Journal of Applied Mechanics*, 1987, Vol. 54, No. 3, pp. 519–524.

Rice, J. R., 1968, "Mathematical Analysis in Mechanics of Fracture," *Fracture: An Advanced Treatise*, Liebowitz, H., ed., Vol. 2, Academic Press, New York, pp. 191–311.

Rice, J. R., 1975, "Elastic-Plastic Models for Stable Crack Growth," *Mechanics and Mechanisms of Crack Growth*, May, M. J., ed., British Steel Corp. Physical Metallurgy Centre Publication, Sheffield, England, pp. 14–39.

Rice, J. R., 1982, "Elastic-Plastic Crack Growth," *Mechanics of Solids*, Hopkins, H. G., and Sewell, M. J., eds., Pergamon Press, Oxford, pp. 539–562.

Rice, J. R., and Sorensen, E. P., 1978, "Continuing Crack-Tip Deformation and Fracture for Plane Strain Crack Growth in Elastic-Plastic Solids," *Journal of Mechanics and Physics of Solids*, Vol. 26, pp. 163–186.

Rice, J. R., Drugan, W. J., and Sham, T. L., 1980, "Elastic-Plastic Analysis of Growing Cracks," *Fracture Mechanics: Twelfth Conference*, ASTM STP 700, American Society for Testing and Materials, pp. 189–221.

Rosakis, A. J., and Freund, L. B., 1982, "Optical Measurement of the Plastic Strain Concentration at a Cracktip in a Ductile Steel Plate," *Journal of Engineering Materials and Technology*, Transactions of ASME, Vol. 104, pp. 115–120.

Schreyer, H. L., Kulak, R. F., and Kramer, J. M., 1979, "Accurate Numerical Solutions for Elastic-Plastic Models," *ASME Journal of Pressure Vessel Technology*, Vol. 101, pp. 226–234.

Sham, T. L., 1983, "A Finite Element Study of the Asymptotic Near-Tip Fields for Mode I Plane Strain Cracks Growing Stably in Elastic-Ideally Plastic Solids," *Elastic-Plastic Fracture: Second Symposium, Volume I—Inelastic Crack Analysis*, ASTM STP 803, Shih, C. F., and Gudas, J. P., eds., American Society for Testing and Materials, Philadelphia, pp. 52–79.

Slepyan, L. I., 1974, "Growing Cracks during Plane Deformation of an Elastic-Plastic Body," *Izv. Akad. Nauk. SSSR, Mekhanika Tverdogo Tela*, Vol. 9, pp. 57–67.

Sorensen, E. P., 1978, "A Finite Element Investigation of Stable Crack Growth in Anti-Plane Shear," *International Journal of Fracture*, Vol. 14, pp. 485–500.

Sorensen, E. P., 1979, "A Numerical Investigation of Plane Strain Stable Crack Growth under Small-Scale Yielding Conditions," *Elastic-Plastic Fracture*, ASTM STP 668, American Society for Testing and Materials, pp. 151–174.

Zehnder, A. T., Rosakis, A. J., and Narasimhan, R., 1986, "Measurement of J Integral with Caustics: An Experimental and Numerical Investigation," Caltech Report SM 86-8, Pasadena, CA.